Vietnam Journal of Science and Technology ***62*** *(4) (2024) 660-669*

doi:10.15625/2525-2518/18302

Synthesis of benzamide derivatives and evaluation of their in vitro and in silico tyrosinase inhibitory activities

Tran Hoai Tu[1, 2], Nguyen Trung Nhan[1, 2], Dang Hoang Phu[1, 2, *]

[1]*Faculty of Chemistry, University of Science, 227 Nguyen Van Cu street, District 5, Ho Chi Minh City, Viet Nam*

[2]*Vietnam National University Ho Chi Minh City, Linh Trung Ward, Thu Duc City, Ho Chi Minh City, Viet Nam*

[*]Email: *dhphu@hcmus.edu.vn*

Received: 27 April 2023; Accepted for publication: 29 December 2023

Abstract. In this research, six benzamide derivatives were traditionally synthesized using hydrazine, carbazide, and hydroxylamine derivatives through the pre- or in situ activation of the carboxylic acid functionality. Their chemical structures were identified as *N*′-phenylbenzohydrazide, *N*′-(2,4-dinitrophenyl)benzohydrazide, *N*′-(benzoyloxy)benzamide, *N*-dibenzoylurea, 2-amino-5-(4-phenyl)-1,3,4-thiadiazole, and benzohydrazide based on the interpretation of NMR spectroscopic data. Among these products, *N*′-phenylbenzohydrazide and *N*-(benzoyloxy)benzamide showed potent tyrosinase inhibitory activity with the IC_{50} values of 10.5 and 2.5 μM, respectively, stronger than that of kojic acid (44.6 μM). Docking studies between *oxy*-tyrosinase and the two active compounds have been carried out to analyze their binding interactions. Both two active compounds showed negative binding free energy values (*S* values) and some more interactions than the positive control (kojic acid). This discovery provided evidence for the potent tyrosinase inhibitory activity of these two compounds, making them promising candidates for the development of anti-tyrosinase agents in medicine and cosmetics.

Keywords: benzamide derivatives, docking studies, tyrosinase inhibitory activity.

Classification numbers: 1.1.2, 1.1.6.

1. INTRODUCTION

Melasma is a common skin pigmentation disorder, particularly prevalent in women in high ultraviolet radiation areas. The disorder is primarily caused by the abnormal accumulation of melanin, a photoprotective biopolymer synthesized by L-tyrosine under the control of tyrosinase [1]. The enzyme tyrosinase (EC 1.14.18.1) is a binuclear copper-containing monooxygenase, which catalyzes the hydroxylation of L-tyrosine to 3,4-dihydroxyphenylalanine (L-DOPA) and L-DOPA to dopaquinones that under unregulated conditions lead to overproduction of melanin pigments [2, 3]. Tyrosinase inhibition is a key target for melasma treatment. Current commercial

tyrosinase inhibitors, such as hydroquinone, ellagic acid, kojic acid, azelaic acid, arbutin, L-ascorbic acid, and tranexamic acid, have drawbacks [4]. Therefore, finding new efficient and safe depigmentation agents, that can be used in cosmetic and skin pigmentation drugs, is necessary.

Amide derivatives offer promise as compounds with multifunctional biological activities such as antituberculosis, anticonvulsant, analgesic, anti-inflammatory, insecticidal, antifungal, and antitumor properties [5]. Scientists recently discovered that amide derivatives, especially benzamides, can also significantly inhibit tyrosinase. Specifically, *N*-(2-hydroxy-ethyl)-3,5-dinitro-benzamide, *N*-(2-bromo-ethyl)-3,5-dinitro-benzamide, *N*-hydroxy-4,*N*-dimethyl-benzamide, *N*-ethyl-benzamide showed strong tyrosinase inhibitory activity with IC_{50} values of 1.09, 3.08, 2.09, 11.83 µg/mL [6], respectively, and stronger than that of the positive control, kojic acid (IC_{50} 16.67 µg/mL) or the discovery of *N*-(acrylolyl)benzamide derivatives showed the inhibition of tyrosinase (% I > 25.99) [7], higher than that of kojic acid (% I = 21.55). Most studies aimed at finding anti-tyrosinase agents are based on benzamide derivatives, synthesized by primary amines [6, 7], and no scientific publications are available for their synthesis using hydrazine, carbazide, and hydroxylamine derivatives. Therefore, our study on finding new anti-tyrosinase agents was carried out, leading to the synthesis of some benzamides by different amines and evaluation of their tyrosinase inhibitory activities. In addition, molecular docking studies of active compounds (**2** and **4**) with the *oxy*-form of the copper-bound tyrosinase were performed.

2. MATERIALS AND METHODS

2.1. Materials

Nuclear Magnetic Resonance (NMR) spectra were performed on a Bruker Avance III 500 spectrometer (Bruker BioSpin AG, Bangkok, Thailand). Chemical shifts were expressed as δ values. The Electrospray Ionization Mass Spectrometry (ESI-MS) were obtained on an Agilent 1260 series single quadrupole Liquid Chromatography/Mass Sectrometry (LC/MS) system (Agilent Technologies, Singapore). Tyrosinase (EC 1.14.18.1) from mushroom (3933 U mL^{-1}) and L-dihydroxyphenylalanine (L-DOPA) were purchased from Sigma-Aldrich (Sigma-Aldrich Pte., Ltd., Singapore). Column chromatography was carried out using silica gel 60, 0.06–0.2 mm (Scharlau, Barcelona, Spain). Kieselgel 60 F_{254} plates for TLC were purchased from Merck (Merck KGaA, Darmstadt, Germany). Other chemicals were of the highest grade available.

2.2. Procedure for the synthesis of amide derivatives

*2.2.1. Synthesis of benzoyl chloride **(1)***

The mixture of benzoic acid (1.0 g, 8.2 mmol) and $SOCl_2$ (3 mL) was refluxed at 80 °C for 1.5 hours. The mixture was continuously heated at 110 °C to evaporate $SOCl_2$, poured into dimethylformamide (DMF), and finally cooled down to obtain the product.

*2.2.2. Synthesis of N'-phenylbenzohydrazide **(2)***

Phenylhydrazine (885.6 mg, 8.2 mmol) and pyridine (648.0 mg, 8.2 mmol) were dissolved in 5 mL of DMF. The mixture was cooled down, and benzoyl chloride (**1**) was added slowly until precipitation. The reaction mixture was stirred for 1.5 hours at room temperature. Then, the mixture was poured into 60 mL of H_2O to precipitate the crude product, which was recrystallized

to MeOH to afford the pure product. *N'*-Phenylbenzohydrazide (**2**): yield 41 %, white solid, m.p. 165 - 168 °C, ESI-MS *m/z* 213.10 $[M+H]^+$, $C_{13}H_{13}N_2O^+$, ^{1}H NMR (acetone-d_6, 500 MHz): δ_H 9.65 (brs, 1H), 7.99 (d, *J* = 7.5 Hz, 2H), 7.58 (t, *J* = 7.5 Hz, 1H), 7.50 (t, *J* = 7.5 Hz, 2H), 7.19 - 7.15 (m, 3H), 6.95 (d, *J* = 7.5 Hz, 2H), 6.78 (t, *J* = 7,5 Hz, 1H), ^{13}C NMR (acetone-d_6, 125 MHz): δ_C 166.6, 149.8, 133.4, 131.6, 128.7, 128.5, 127.3, 119.7, 113.2 [8].

2.2.3. Synthesis of N'-(2,4-dinitrophenyl)benzohydrazide ***(3)***

2,4-Dinitrophenylhydrazine (1640.0 mg, 8.2 mmol) and pyridine (648.0 mg, 8.2 mmol) were dissolved in 10 mL of DMF. The mixture was cooled down, and then benzoyl chloride (**1**) was added slowly until an orange precipitate formed. The mixture was stirred for 1.5 hours at room temperature and then poured into 60 mL of H_2O to precipitate the crude product, which was recrystallized to MeOH. Finally, column chromatography was used with EtOAc: *n*-hexane (40 % *n*-hexane) to purify the product. *N'*-(2,4-Dinitrophenyl)benzohydrazide (**3**): yield 36 %, black solid, m.p. 213 - 215 °C, ESI-MS *m/z* 303.07 $[M+H]^+$, $C_{13}H_{11}N_4O_5^+$, ^{1}H NMR (acetone-d_6, 500 MHz): δ_H 10.08 (s, 1H), 9.03 (d, *J* = 2.6 Hz, 1H), 8.36 (dd, *J* = 9.5, 2.6 Hz), 8.05 - 7.96 (m, 2H), 7.70 - 7.47 (m, 4H) [9].

2.2.4. Synthesis of N-(benzoyloxy)benzamide ***(4)***

Hydroxylamine hydrochloride (569.9 mg, 8.2 mmol) and pyridine (1296.0 mg, 16.4 mmol) were dissolved in 10 mL of DMF. The mixture was refluxed at 70–80 °C, and benzoyl chloride (**1**) was added slowly until precipitation. The reaction mixture was poured into 60 mL of cool H_2O to precipitate the crude product, which was recrystallized into MeOH to obtain the pure product. *N*-(Benzoyloxy)benzamide (**4**): yield 36 %, white solid, m.p. 157 - 160 °C, ESI-MS *m/z* 242.08 $[M+H]^+$, $C_{14}H_{12}NO_3^+$, ^{1}H NMR (acetone-d_6, 500 MHz): δ_H 8.14 - 8.12 (m, 2H), 7.96 - 7.94 (m, 2H), 7.74 (td, *J* = 7,5; 1,1 Hz, 1H), 7.64 - 7.59 (m, 3H), 7.55 - 7.52 (m, 2H) [10].

2.2.5. Synthesis of N-dibenzoylurea ***(5)***

Urea (492.0 mg, 8.2 mmol) and pyridine (648.0 mg, 8.2 mmol) were dissolved in 5 mL of DMF. The mixture was cooled down, and benzoyl chloride (**1**) was added slowly until precipitation. The reaction mixture was stirred for 1.5 hours at room temperature. Then, the mixture was poured into 60 mL of $NaHCO_3$ to precipitate the product, which was washed with Na_2CO_3 to obtain the product. *N*-carbamoylbenzamide (**5**): yield 40 %, white solid, m.p. 205 - 208 °C, ESI-MS *m/z* 269.09 $[M+H]^+$, $C_{15}H_{13}N_2O_3^+$, ^{1}H NMR (acetone-d_6, 500 MHz): δ_H 8.05 - 8.03 (d, *J* = 8.5 Hz, 2H), 7.65 - 7.60 (m, 2H), 7.51 - 7.48 (m, 2H) [11].

2.2.6. Synthesis of 2-amino-5-(4-phenyl)-1,3,4-thiadiazole ***(6)***

Benzoic acid (1220.2 mg, 10.0 mmol) and thiosemicarbazide (910.0 mg, 10.0 mmol) were dissolved in 5 mL of $POCl_3$. The mixture was refluxed at 70 - 80 °C for 3 hours, and then 25 mL of H_2O was added. The reaction mixture was continuously refluxed at 70 °C for 2.5 hours, and KOH solution was added until precipitating the crude product, which was recrystallized into EtOH to afford the pure product. 2-Amino-5-(4-phenyl)-1,3,4-thiadiazole (**6**): yield 65 %, yellow solid, m.p. 223 - 227 °C, ESI-MS *m/z* 196.05 $[M+H]^+$, $C_8H_{10}N_3SO^+$, ^{1}H NMR (Dimethylsulfoxide-d_6 (DMSO-d_6), 500 MHz): δ_H 7.74 - 7.72 (dd, *J* = 8.2, 1.5 Hz, 2H), 7.46 - 7.40 (m, 3H), 7.37 (s, 2H), ^{13}C NMR (DMSO-d_6, 125 MHz): δ_C 169.0, 156.9, 131.5, 130.0, 129.6, 126.8 [12].

2.2.7. Synthesis of benzohydrazide ***(7)***

Hydrazine sulfate (10.0 g, 0.077 mol) and NaOH (8.0 g, 0.200 mol) were dissolved in 10 mL of H_2O. The mixture was heated by simple distillation at 70 °C for 30 minutes and then at 150 °C for 1.5 hours to afford hydrazine hydrate. Benzoic acid (1.5 g, 0.012 mol) and 98 % sulfuric acid (0.5 mL) were dissolved in 4 mL of MeOH. The mixture was refluxed at 70 °C for 2 hours and then extracted with H_2O and diethyl ether to obtain methyl benzoate. Hydrazine hydrate, methyl benzoate, and 5 mL of MeOH mixture were refluxed at 70 °C for 2 hours. The reaction mixture was poured into cool water and recrystallized into MeOH to afford the pure product. Benzohydrazide (**7**): yield 14 %, white solid, m.p. 111 - 115 °C, ESI-MS *m/z* 137.07 $[M+H]^+$, $C_7H_9N_2O^+$, ^{1}H NMR (DMSO-d_6, 500 MHz): δ_H 9.73 (s, 1H), 7.80 (d, J = 7.1 Hz, 2H), 7.50 - 7.47 (m, 1H), 7.44 - 7.41 (m, 2H), 4.54 (s, 2H) [13].

2.3. Tyrosinase inhibitory assay

The tyrosinase inhibitory activity assay was performed as previously described by Dang *et al*. [14]. Test mixtures including 1900 μL of test solution and 100 μL of tyrosinase solution (15 U/mL) were prepared at pH 6.8 in 0.1 M phosphate buffer and preincubated for 30 minutes at room temperature. These mixtures were added with 1000 μL of 1.5 mM L-DOPA, which were then kept in phosphate buffer at pH 6.8 and continuously incubated for 7 minutes at room temperature. Shimadzu UV-1800 spectrophotometer was used for determining the absorbance (A) at 475 nm. The term inhibitory percentage (I %) is a measure of how much a specific substance or compound inhibits or reduces enzymatic activity. It quantifies the extent of inhibition, typically expressed as a percentage, by comparing the enzymatic activity in the presence and absence of the inhibitor. The I% values were calculated as follows: $\mathbf{I}\% = \frac{A_{\mathbf{control}} - A_{\mathbf{sample}}}{A_{\mathbf{control}}} \times \mathbf{100}\,\%$. Data were described as means ± standard error ($n = 3$). Multivariate nonlinear regression and $R^2 > 0.9$ in GraphPad Prism software were used to determine the IC_{50} values. The positive control in this assay was kojic acid.

2.4. Molecular docking

The molecular docking was performed as previously described by Dang *et al*. [14]. A Molecular Operating Environment 2016 (MOE 2016.0802) suite was used for docking studies of 2, 3, kojic acid (the positive reference), and hypoxanthine (the decoy). The Builder module was used to construct the chemical structures of these compounds, and then the all-atom forcefield combining EHT (Extended Hueckel Theory) and Amber12 (Assisted Model Building with Energy Refinement) were applied to minimize these compounds up to 0.0001 gradients. The PLB (Propensity for Ligand Binding) score in the Site Finder module was used to find the binding site. The *oxy*-tyrosinase structure (PDB code 1WX2) was chosen from the Protein Data Bank, and then water molecules and the caddie protein (ORF378) were detached. The molecular docking was carried out by the Dock module, using the Triangle Matcher placement, Induced Fit refinement, London dG, and GBVI/WSA dG scoring methods. The best pose was taken from the five top poses with the lowest binding free energy value (S value) to analyze the receptor-ligand interactions using a BIOVIA Discovery Studio Visualizer 2016.

3. RESULTS AND DISCUSSION

3.1. Synthesis of amine derivatives

*3.1.1. Synthesis of benzoyl chloride (**1**)*

Briefly, amide derivatives were prepared by the reaction between benzoic acid and amine. However, the preparation of amides by direct reaction of carboxylic acids with amines is challenging because amines are bases that convert acidic carboxyl groups to their unreactive carboxylate anions ($RCOO^-$) [15]. The better and non-acidic leaving group must replace the hydroxy group; therefore, benzoic acid was converted to benzoyl chloride (**1**). Since 1 is unstable, its structure was determined by TLC instead of NMR data.

*3.1.2. Synthesis of benzohydrazide derivatives (**2**, **3**)*

In this study, nucleophilic substitution was carried out to synthesize amide derivatives (Figure 1). The synthesis of *N*′-phenylbenzohydrazide (**2**) was performed by phenylhydrazine and pyridine in 5 mL of DMF. **1** was added slowly to the cool reaction mixture to prevent the outcome of over-acylation, which is the reaction between amides and **1**. The mixture was poured into 60 mL of H_2O to precipitate the crude product, which was recrystallized into MeOH to afford the pure product. The structure was elucidated through determination by NMR spectroscopy. The ^{1}H NMR spectrum of **2** displayed signals at δ_H 6.78 - 8.00 for two phenyl groups and at δ_H 9.65 for an amide group. The ^{13}C NMR showed signals at δ_C from 113.2 to 149.8 for a phenyl group and at δ_C 166.6 for a carbonyl group.

The procedure for the synthesis of *N*′-(2,4-dinitrophenyl)benzohydrazide (**3**) is similar to that of **2**. However, 2,4-dinitrophenylhydrazine is hard to dissolve in DMF; therefore, 10 mL of DMF was used to increase the dissolving ability. The ^{1}H NMR spectrum of **3** showed signals at δ_H 7.47 - 9.03, indicating a phenyl group and a 2,4-dinitrobenzene ring and at δ_H 10.08 for an amide group.

*3.1.3. Synthesis of N-(benzoyloxy)benzamide (**4**)*

The synthesis of *N*-(benzoyloxy)benzamide (4) is the same as that of **2** (Figure 1). Hydroxylamine is stored as the hydroxylammonium hydrochloride salt ($NH_2OH.HCl$), so the reaction was carried out by the reflux method. Moreover, the volume of pyridine was much more than that in the synthesis of **2** to convert from the salt form to a free amine.

Since the nucleophilicity of the amino group was higher than that of the hydroxyl group, it reacted with **1** to form **4**′. Besides, **4**′ continuously reacted to form **4**. The ^{1}H NMR spectrum of **4** showed signals of 10 aromatic protons at δ_H from 7.00 to 8.00, with two phenyl groups.

*3.1.4. Synthesis of N-dibenzoylurea (**5**)*

N-Dibenzoylurea (**5**) was synthesized similarly to **2** (Figure 1). However, in the crystallization process, $NaHCO_3$, instead of H_2O, was used to precipitate the crude product which was then washed with Na_2CO_3 to obtain the pure product. The ^{1}H NMR spectrum of **5** showed signals of aromatic protons at δ_H from 7.50 to 8.00, with two phenyl groups.

*3.1.5. Synthesis of 2-amino-5-(4-phenyl)-1,3,4-thiadiazole (**6**)*

The synthesis of 2-amino-5-(4-phenyl)-1,3,4-thiadiazole (**6**) was performed in $POCl_3$. The expected product in this reaction was the formation of amide linkage (**6**′). However, the **6**′ was quickly transformed into a Schiff base [16] through the replacement of the carbonyl group with an imine group, containing a carbon-nitrogen double bond. Then, the hydroxyl group was converted into the better-leaving group -$OPOCl_2$, with the attendance of $POCl_3$, which resulted in the formation of a thiadiazole ring (Figure 2). The ^{1}H NMR spectrum of **6** displayed signals of

a phenyl group at δ_H 7.40 - 7.74, and the signal of NH_2, directly attached to an aromatic ring, at δ_H 7.37. The ^{13}C NMR showed the signals of 6 carbons at δ_C 126.8 - 169.0.

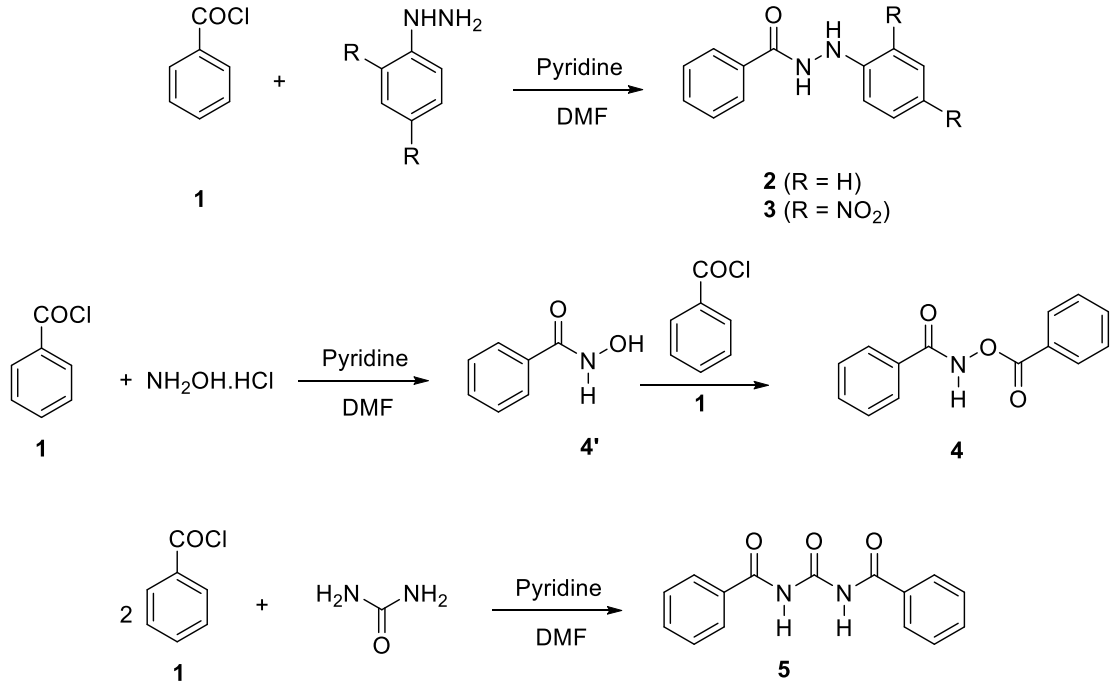

Figure 1. Synthesis of *benzamide derivatives **2–5***.

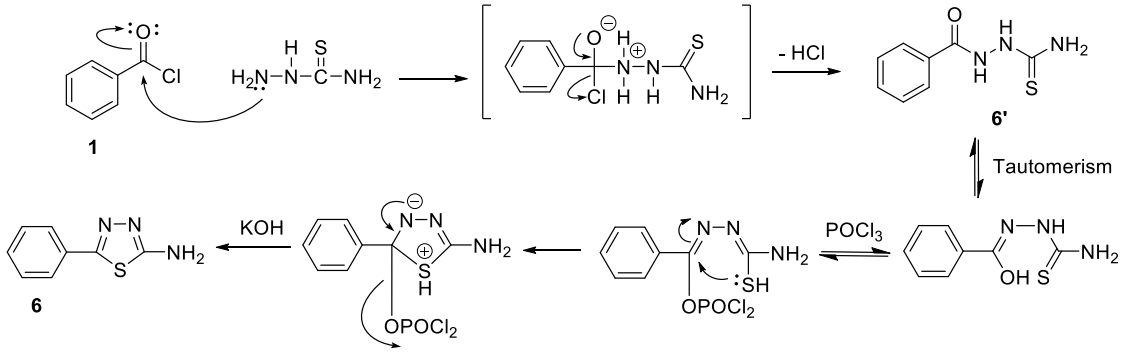

Figure 2. Reaction mechanism of 2-amino-5-(4-phenyl)-1,3,4-thiadiazole **(6)**.

*3.1.6. Synthesis of benzohydrazide **(7)***

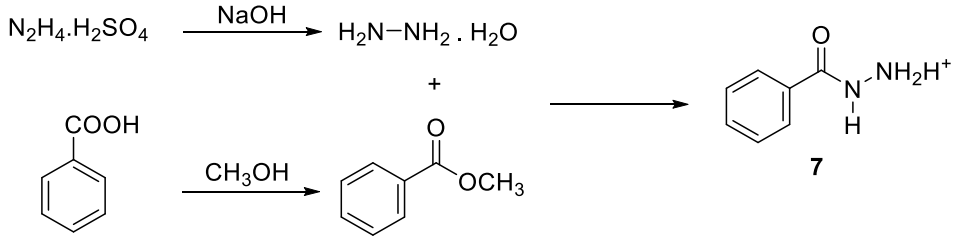

Figure 3. The synthesis of benzohydrazide **(7)**.

Since hydrazine sulfate is stored as a salt and is insoluble in organic solvents, the reaction converting it to active hydrazine hydrate was carried out. The synthesis of benzohydrazide (**7**) was performed in the presence of methyl benzoate instead of benzoyl chloride because benzoyl chloride is quickly deactivated by water (Figure 3). The ^{1}H NMR spectrum of **7** displayed signals at δ_H 7.41 - 7.80, indicating the formation of a phenyl group, and at δ_H 9.73 and 4.54 for an amide group and an amine group, respectively.

3.2. Evaluation of tyrosinase inhibitory activity

Synthesized amine derivatives were tested for their tyrosinase inhibitory activity. A positive control for this assay was kojic acid, a current purported skin-lightening agent. *N*′-phenylbenzohydrazide (**2**) and *N*-(benzoyloxy)benzamide (**4**) exhibited remarkable activity with IC_{50} values of 10.5 and 2.5 μM, respectively, demonstrating higher potential than kojic acid (IC_{50} of 44.6 μM) (Table 1).

Table 1. Tyrosinase inhibitory of amine derivatives.

	I%				**IC_{50} (μM)**
Compound	**100 μM**	**50 μM**	**25 μM**	**10 μM**	
2	98.71 ± 0.50	89.72 ± 0.50	77.61 ± 0.80	49.09 ± 0.90	10.5
3	6.43 ± 0.70	–	–	–	> 100
6	15.47 ± 0.72	5.97 ± 0.98	–	–	> 100
7	28.94 ± 0.86	25.57 ± 0.82	22.97 ± 0.34	14.40 ± 0.89	> 100
	10 μM	**5 μM**	**2.5 μM**	**1 μM**	
4	90.17 ± 0.50	73.22 ± 0.87	50.48 ± 0.61	21.39 ± 0.65	2.5
5	–	–	–	–	> 100
Kojic acid[a]					44.6

[a]Positive control: I% < 1 %.

3.3. Docking study of active compounds 2, 4

The four possible oxidation states of tyrosinase are *deoxy*, *oxy*, *met*, and *deact* forms [17]. *Met*-tyrosinase, with two Cu^{2+} ions and one hydroxy in the binding site, is accountable for the oxidation of catechols, which means that two Cu^{2+} ions are converted to the Cu^{1+} oxidation state of *deoxy*-tyrosinase. *Deoxy*-tyrosinase binds to dioxygen to form the oxy-tyrosinase state, which is the primary form of the enzyme with a peroxide group bridging two Cu^{2+} ions. The peroxide group and two bound Cu^{2+} ions of *oxy*-tyrosinase play an important role in catalytic oxidation. Mushroom tyrosinase (EC 1.14.18.1) used in the inhibitory assay is similar to *oxy*-tyrosinase form. Therefore, **2** and **4** were used in molecular docking studies with *oxy*-tyrosinase (PDB ID : 1WX2) [18] to clarify the inhibition mechanisms and their interactions.

In molecular docking studies, active and decoy ligands (imperfect scoring results), which can happen by applying nonbinding molecules or predicting wrong ligand geometries, are the same in physical and chemical properties such as total hydrogen bond donors, total hydrogen bond acceptors, molecular weight, number of rotational bonds, octanol-water partition coefficient, and topological polar surface area. However, the decoy is assumed to be inactive against the target. According to Choi [19], the tyrosinase inhibitory constant (K_i) values of hypoxanthine and kojic acid are >1000 and 13 μM, respectively. In this study, the decoy

molecule and the active inhibitor were hypoxanthine and kojic acid to validate our docking protocol.

Table 2. Docking results of **2**, **4**, kojic acid, and hypoxanthine with *oxy*-tyrosinase.

	oxy-Tyrosinase (1WX2)			
Compound	***S* value**	**Interaction**	**Targeting residue**	**Distance (Å)**
2	–5.14	π-π	HIS194	5.45
		π-π	HIS194	4.52
		π-cation	HIS194	4.88
			ARG55	3.39
		π-alkyl	ILE42	4.24
		H-donor	ASN191	2.12
4	–5.63	π-π	HIS194	3.52
			HIS54	5.77
		π-cation	ARG55	3.50
		π-alkyl	ILE42	4.47
		H-donor	ASN191	2.98
Kojic acid	–4.66	H-donor	PER404	3.08
			THR203	2.03
		π-π	HIS194	3.85
		Metal-donor	Cu^{2+}	3.18
Hypoxanthine	–4.47	H-donor	PER404	2.75

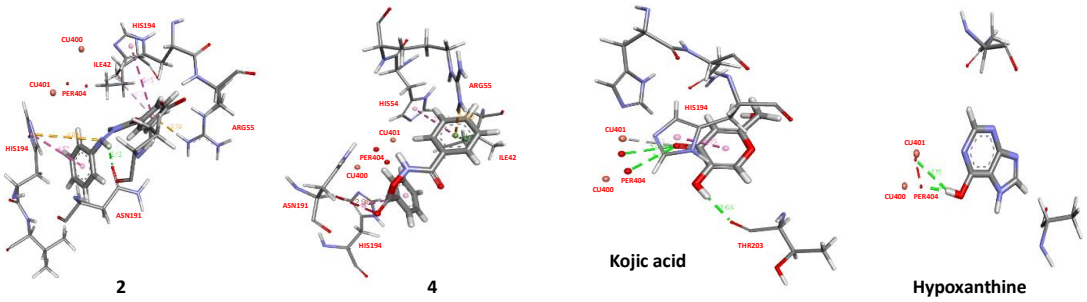

Figure 4. Docked pose of best-ranked docking score of compounds 2, 4, kojic acid, and hypoxanthine.

A Molecular Operating Environment 2016 (MOE 2016.0802) suite was applied for docking studies [20]. Then a BIOVIA Discovery Studio Visualizer 2016 was used to choose the top-ranked pose having the lowest binding free energy value (*S* value) [21]. The *S* values and the number of interactions of **2**, **4**, and kojic acid proved that **2** and **4** could be potential inhibitors of *oxy*-tyrosinase based on their higher binding affinity than kojic acid (Table 2), which was suitable for their experimental inhibitory activities (**2**, **4** > kojic acid). In addition, compounds **2** and **4** showed π-π interactions between their aromatic groups, HIS194 and HIS54 (these are amino acid groups bound around the active site), with the distance ranging from 3.52 to 5.77 Å, respectively (Figure 4). Both compounds **2** and **4** exhibited π-cation interactions with ARG55 residue, π-alkyl interactions with ILE42 residue, and H-donor interactions with ASN191. Moreover, **4** showed an *S* value lower than that of **2**, with their *S* values being –5.63 and –5.14, respectively. That demonstrated why the tyrosinase inhibitory activity of **2** was weaker than that

of **4**. Hypoxanthine indicated the highest *S* value and only the distance of H-donor interaction with PER404.

4. CONCLUSIONS

In conclusion, our study aimed to discover novel anti-tyrosinase agents through the synthesis of various benzamides using different amines, followed by the evaluation of their tyrosinase inhibitory activities. Among the compounds synthesized, compounds **2** and **4** emerged as standout candidates, exhibiting significant tyrosinase inhibitory activities with IC_{50} values of 10.5 µM and 2.5 µM, respectively. These results suggest that compounds **2** and **4** hold promise as lead molecules for the further development of anti-tyrosinase agents. Furthermore, molecular docking studies were conducted to gain insights into the interactions between active compounds and the *oxy*-form of copper-bound tyrosinase. The docking results highlighted that compounds **2** and **4** exhibited notably stronger binding affinities for *oxy*-tyrosinase than kojic acid. This finding supports the potential of compounds **2** and **4** as effective tyrosinase inhibitors, making them attractive targets for further development in the quest to create effective anti-tyrosinase agents for various applications in medicine and cosmetics. Further research and optimization of these compounds may lead to the development of novel therapies for conditions associated with aberrant tyrosinase activity.

Acknowledgements. This research was funded by the University of Science - Vietnam National University Ho Chi Minh City (VNU-HCM) under grant no. T2022-63.

CRediT authorship contribution statement. Nguyen Trung Nhan: Investigation, formal analysis. Tran Hoai Tu: Supervision, formal analysis, and writing the manuscript. Dang Hoang Phu: Investigation, formatting and submitting the final manuscript.

Declaration of competing interest. The authors declare that there are no conflicts of interest regarding the publication of this paper.

REFERENCES

1. Chawla S., Delong M. A., Visscher M. O., Wickett R. R., Manga P., Boissy R. E. - Mechanism of tyrosinase inhibition by deoxyArbutin and its second-generation derivatives, Br. J. Dermatol. **159** (2008) 1267-1274. doi.org/10.1111/j.1365-2133.2008.08864.x.
2. Rodriguez-Lopez J. N., Tudela J., Varon R., Garcia-Carmona F., Garcia-Canovas F. - Analysis of a kinetic model for melanin biosynthesis pathway, J. Biol. Chem. **267** (1992) 3801-3810. doi.org/10.1016/S0021-9258(19)50597-X.
3. Decker H., Tuczek F. - Tyrosinase/catecholoxidase activity of hemocyanins: structural basis and molecular mechanism, Trends. Biochem. Sci. **25** (2000) 392-397. doi.org/10.1016/s0968-0004(00)01602-9.
4. Pillaiyar T., Manickam M., Namasivayam V. - Skin whitening agents: medicinal chemistry perspective of tyrosinase inhibitors, J. Enzyme Inhib. Med. Chem. **32** (2017) 403-425. doi.org/10.1080/14756366.2016.1256882.
5. Kushwaha N., Saini R. K., Kushwaha S. K. - Synthesis of some amide derivatives and their biological activity, Int. J. ChemTech. Res. **3** (2011) 203-209.

6. Khan S. B., Khan M. T. H., Jang E. S., Akhtar K., Seo J., Han H. - Tyrosinase inhibitory effect of benzoic acid derivatives and their structure-activity relationships, J. Enzyme Inhib. Med. Chem. **25** (2010) 812-817. doi.org/10.3109/14756366.2010.482529.
7. Lee S., Ullah S., Park C., Lee H. W., Kang D., Yang J., Akter J., Park Y., Chun P., Moon H. R. - Inhibitory effects of *N*-(acryloyl)benzamide derivatives on tyrosinase and melanogenesis, Bioorg. Med. Chem. **27** (2019) 3929-3937. doi.org/10.1016/ j.bmc.2019.07.034.
8. Gallagher N., Zhang H., Junghoefer T., Giangrisostomi E., Ovsyannikov R., Pink M., Rajca S., Casu M. B., Rajca A. - Thermally and magnetically robust triplet ground state diradical, J. Am. Chem. Soc. **141** (2019) 4764-4774.
9. Catarzi D., Cecchi L., Colotta V., Melani F., Filacchioni G., Martini C., Giusti L., Lucacchini A. - Tricyclic heteroaromatic systems 1,2,4-triazolo[1,5-a]quinoxalines: synthesis and benzodiazepine receptor activity. Farmaco. **48** (1993) 1065-1078.
10. Guimond N., Gorelsky S. I., Fagnou K. - Rhodium(III)-Catalyzed Heterocycle Synthesis Using an Internal Oxidant: Improved Reactivity and Mechanistic Studies. J. Am. Chem. Soc. 133 (2011) 6449-6457.
11. Hernandez A. G., Grooms G. M., El-Alfy A. T., Stec J. - Convenient one-pot two-step synthesis of symmetrical and unsymmetrical diacyl ureas, acyl urea/carbamate/thiocarbamate derivatives, and related compounds. Synthesis. **49** (2017) 2163-2176.
12. Hatvate N. T., Ghodse S. M., Telvekar V. N. - Metal-free synthesis of 2-aminothiadiazoles via TBHP-Mediated oxidative C-S bond formation. Synth Commun. **48** (2018) 285-290.
13. Liu K. J., Jiang S., Lu L. H., Tang L. L., Tang S. S., Tang H. S., Tang Z., He W. M., Xu X. - Bis(methoxypropyl) ether-promoted oxidation of aromatic alcohols into aromatic carboxylic acids and aromatic ketones with O_2 under metal- and base-free conditions. Green Chem. **20** (2018) 3038-3043.
14. Dang P. H., Le, T. H., Do, T. N. V., Nguyen, H. X., Nguyen, M. T. T., & Nguyen, N. T. - Diarylalkanoids as potent tyrosinase inhibitors from the stems of *Semecarpus caudata*, Evid. Based Complement. Alternat. Med., **2021** (2021) 8872920. doi:10.1155/ 2021/8872920.
15. McMurry J. - Organic Chemistry, 9th ed., Cornell University, United States (2015).
16. Isabella R., Giorgio F. - Different Schiff bases−Structure, importance and classification, Molecules. **27** (2022) 787-795. doi.org/10.3390/molecules27030787.
17. Christopher A. R., Patrick A. R. - Tyrosinase: The four oxidation states of the active site and their relevance to enzymatic activation, oxidation and inactivation, Bioorg. Med. Chem. **22** (2014) 2388-2395. doi.org/10.1016/j.bmc.2014.02.048.
18. Matoba Y., Kumagai T., Yamamoto A., Yoshitsu H., Sugiyama M. - Crystallographic evidence that the dinuclear copper center of tyrosinase is flexible during catalysis, J. Biol. Chem. **281** (2006) 8981-8990. doi.org/10.1074/jbc.M509785200.
19. Choi J., Lee Y. M., Jee J. G. - Thiopurine drugs repositioned as tyrosinase inhibitors, Int. J. Mol. Sci. **19** (2018) 77-92. doi.org/10.3390/ijms19010077.
20. Chemical Computing Group. - Molecular operating environment (MOE) 2016, Chemical Computing Group, Montreal, QC, Canada, 2016.
21. Dassault Systèmes BIOVIA. - BIOVIA Discovery Studio Visualizer, Dassault Systèmes BIOVIA, San Diego, CA, USA, 2016.